Strategic design and development of a siderophore mimic: Pioneering anticancer therapy via ROS generation and ferroptosis

Abhishek Panwar,[a] Anushree Lye,[b] Dulal Musib,[a] Aarti Upadhyay [c], Irungbam Karankumar,[a] Paonam Bebika Devi,[a] Maynak Pal,[a] Biswanath Maity,[b]* and Mithun Roy[a,d]*

a) Department of Chemistry, National Institute of Technology Manipur, Langol-795004, Imphal West, Manipur (INDIA).

b) Department of Systems Biology, Center of Biomedical Research (CBMR), Raebareli Road, Lucknow 226014, Uttar Pradesh, India

c) Department of Inorganic and Physical Chemistry, Indian Institute of Science Bangalore, Bangalore-50012, Karnataka (INDIA).

d) Department of Chemistry, National Institute of Technology Agartala, Jirania, West Tripura, Pin – 799046 (INDIA)

Supporting Information

Table of Contents		**Page No**

Methods and Materials

$[Fe(NO_3)_3.9H_2O]$, $FeCl_2.4H_2O$, 1H-pyrrole, 4-methyl benzaldehyde, propionic acid, triethylamine, trifluoroacetic acid (TFA), L-dopa, EDC.HCl, HOBT, Di-*tert*-butyl dicarbonate, MTT, BSA, 1,10-phenanthroline, sodium hydroxide, 2′,7′-Dichlorofluorescin diacetate (CM-H2DCFDA) and sodium chloride were purchased from Sigma-Aldrich (USA). Dopamine.HCl, L-ascorbic acid, Glutathione reduced (GSH) and DTNB were purchased from SRL Chemical Company (India). L-15 Media (Lonza), DMEM media (MP Biomedicals), Penicillin (Gibco), Streptomycin (Gibco), Fetal Bovine Serum (Gibco), Trypsin EDTA (Sigma-Aldrich), 6 well plates (Tarsons), Nunclon Sphera 3D Ultra-Low Attachment Microplate 96-well Clear Round Bottom (Thermo-Fisher Scientific), MTT Reagent (Invitrogen), Cell culture grade DMSO (MP Biomedicals). Other chemicals and solvents were purchased fro±m TCI Chemicals, Alfa-Aesar, HI-MEDIA, and Finnar Chemicals and used without further purification. The solvents used were purified according to reported protocols prior to their use[1].

UV-visible spectra of the compounds and UV-visible spectroscopic experiments were performed using a Perkin-Elmer UV-visible spectrophotometer. The IR spectra were recorded using a Perkin-Elmer UATR Two FT-IR spectrophotometer. Cyclic voltammetry studies were performed using Metrohm Autolab Potentiostat. The Q-TOF-ESI mass spectra were recorded using Bruker Esquire 3000. DCFDA and Annexin-V/PI assays were studied by fluorescence-activated cell sorting (FACS) analysis using BD FACSVerse Flow Cytometer.

Binding constant studies[2]

We have calculated the binding constant or formation constant of the [**Fe-(III)_T-CATL**] complex by following a previously published protocol.[2] The binding constant was determined by doing UV-visible spectrophotometric titrations in 5% DMSO-PBS buffer at pH 7.4, in which different concentration of ferric ion was added to the ligand in a 1:1 stochiometry until it got into an equilibrium position, the K value was determined by using the Benesi-Hildebrand method, i.e.

Using the stoichiometry 1:1 the association constant can be calculated as follows:

$$\mathbf{M + L \leftrightarrows ML} \qquad (1)$$

$$\mathbf{K = \frac{[ML]}{[M]\,[L]}} \qquad (2)$$

According to the benesi-Hildebrand method, the relation to calculate the binding constant for a 1:1 stochiometry is given as follows:

$$\text{Log}\left(\frac{A - A_0}{A_f - A_0}\right) = \text{Log}\,[Fe^{3+}] + \text{Log}\,K_b$$

in which A_0, A, and A_f are the absorption values, in the absence of, at the intermediate and the saturation of the interaction of Fe^{3+} ion respectively, and $[Fe^{3+}]$ represents the concentration of aqueous Fe^{3+} ion added. The binding constant (K_b = 1.5 x 10^{14} M^{-1}) was determined by linear fitting of the absorption titration curve.

Chelation Studies

We have explored the leaching of iron from the **Fe-TPP-Cl** complex by using tris-catecholate ligand (**T-CATL**). The leaching of iron was investigated by UV-visible titrations in 5% DMSO-PBS buffer at pH 5.5 and 7.4. The chelating ligand (**T-CATL**) was used as the titrant to react with **Fe-TPP-Cl** complex. Initially, we prepared two stock solutions, each with a concentration of 1 millimolar (mM), of the ligand (**T-CATL**) and **Fe-TPP-Cl** in DMSO. After that, we did the titration studies in 5% DMSO-PBS buffer by taking **Fe-TPP-Cl** (75µL) of concentration 0.3mM in the cuvette and then slowly titrating it with varying concentrations of ligand (**T-CATL**) 3.75µL (0.05 eq), 11.25 µL (0.15 eq), 15 µL (0.2 eq), 18.75 µL (0.25 eq), 22.5 µL (0.3 eq), 33.75 µL (0.45 eq), 37.5 µL (0.5 eq), 75 µL (1eq). On gradually increasing the concentration of ligand, there was the formation of a new Q band at around 665 nm whose origin was mainly due to $\pi-\pi^*$ transition in a free protonated porphyrin (H_2TPP) i.e, when the iron is out from the porphyrin core.[3] Subsequently, we also observed another peak at around 570 nm (newly generated LMCT band) indicating the chelation of iron by catecholate ligand.

Glutathione as reducing environment[4]

We have used glutathione as a reducing agent to explore the release of unbound iron from the iron-catecholate complex **$(Fe^{III}T\text{-}CATL)^{3-}$**. As in our present study, we want to show the release of iron after the iron gets leached out from metalloprotein (**Fe-TPP-Cl**) via catecholate ligand (**T-CATL**) which results in the formation of an iron-catecholate complex. Therefore, to show the releasing studies of iron in the presence of glutathione, we have synthesized and characterized **$(Fe^{III}T\text{-}CATL)^{3-}$** complex which was used as a model to show the release of unbound iron in the presence of GSH. The release of unbound iron was investigated by UV-visible titrations in 5% DMSO-PBS buffer at pH 5.5 and 7.4. For this study, we prepared two stock solutions, one with a concentration of 1 mM of complex **$(Fe^{III}T\text{-}CATL)^{3-}$** and another 30 mM of **GSH** in DMSO. After that, we did the titration studies in 5% DMSO-PBS buffer by taking **$(Fe^{III}T\text{-}CATL)^{3-}$** complex (120 µL) of concentration 0.06 mM in the cuvette and then slowly titrating it with varying concentrations of GSH as 0.1 mM, 0.5 mM, 1.0 mM, 2.0 mM, 4.0 mM, 6.0 mM, 8.0 mM, and 10 mM. Using GSH as a reducing environment, we observed a decrease in absorbance of the LMCT band at around 570 nm, which showed that our **$(Fe^{III}T\text{-}CATL)^{3-}$** complex was either getting degraded or the iron metal was getting unbounded from the ligand.

Fe^{+2} releasing studies in the presence of GSH[5,6]

After confirming the release of iron from our previous glutathione studies, we explored our study further to check the presence of unbound iron as Fe^{+2}. Therefore to know the release of unbound iron as Fe^{+2} we have done UV-visible titrations in 5% DMSO-PBS buffer at pH 5.5 and 7.4. For this study, we prepared three different stock solutions, one with a concentration of 1 mM of **$(Fe^{III}T\text{-}CATL)^{3-}$** complex, another with a concentration of 1 mM of 1,10-phenanthroline, and the last with a concentration of 30 mM of **GSH** in DMSO. Firstly, we have taken **$(Fe^{III}T\text{-}CATL)^{3-}$** complex (1 eq) (100 µL) and phenanthroline (3 eq) (280 µL) together in the cuvette. After observing no change we started titrating the mixture with varying concentrations of glutathione(GSH) as 0.1 mM, 0.5 mM, 1.0 mM, 2.0 mM, 4.0 mM, 6.0 mM, 8.0 mM, and 10 mM in both pH (5.5 and 7.4). In this study, phenanthroline ligand was used as a probe for knowing the presence of Fe^{+2} ion as it has a greater affinity for Fe^{+2} ion and forms a stable Fe(II)-tris-phenanthroline complex giving a red color. Hence, after increasing GSH concentrations in the presence of phenanthroline (3 eq) and **$(Fe^{III}T\text{-}CATL)^{3-}$** complex (1 eq), we have observed a new peak formation at 515 nm which corresponds to the MLCT transitions by Iron(II)phenanthroline complex while the peak at 570 nm corresponds to the LMCT transition for **$(Fe^{III}T\text{-}CATL)^{3-}$** complex which gets degraded upon increasing the concentration of GSH. The peak at 515 nm was found to be a characteristic MLCT peak of Fe(II)-tris phenanthroline complex, which was also confirmed by red solution in the cuvette and also by reported literature.[5] This new peak at 515 nm confirmed that the **$(Fe^{III}T\text{-}CATL)^{3-}$** complex in the presence of GSH gets unbounded as Fe^{+2}. After knowing that the iron was unbounded as Fe^{+2} we have determined the normalized percentage release of Fe^{+2} with respect to different concentrations of GSH through a calibration curve plot of Fe(II)tris-phenanthroline complex. We have observed that the percentage release of Fe^{+2} in pH 5.5 was around 83% while in pH 7.4 it was coming as 80%. Reductive release of iron from the **$(Fe^{III}T\text{-}CATL)^{3}$** complex was also confirmed by cyclic voltammetric assays in which a dimethyl formamide (DMF) solution of the **$(Fe^{III}T\text{-}CATL)^{3-}$** complex (0.3 mM) in the presence of 1,10-phenanthroline (0.6 mM) and using 0.1 M TBAP (tetrabutylammonium perchlorate) as the supporting electrolyte, with glassy carbon serving as the working electrode, Ag/AgCl as the reference electrode, and Pt as the counter electrode was used. In this mixture, GSH was added in an increasing concentration as 0.1 mM, 0.5 mM, 1.0 mM, 2.0 mM, 4.0 mM, 6.0 mM, 8.0 mM, and 10 mM, and cyclic voltammetric responses were recorded with a scan rate of 50 mVs^{-1}. We observed the development of characteristic peak potentials of $[Fe(phen)_3]^{2+}$ at 1.3 V and 1.2 V.[6] The

electrochemical assays provide further evidence that in the presence of GSH, the **(Fe^{III}T-CATL)$^{3-}$** releases iron in the form of Fe^{2+}.

Hydroxyl radical generation study[7,8,9]

We evaluated the generation of hydroxyl radicals by trapping them by the formation of salicylic acid from benzoic acid (0.2 mM) by UV-visible spectrophotometry. In this study, firstly, we incubate [$Fe(NO_3)_3.9H_2O$] (0.2 mM), benzoic acid (0.2 mM), and **(Fe^{III}T-CATL)$^{3-}$** complex (0.03mM) both in the sample and the reference cuvette in 5% DMSO-PBS buffer at pH 7.4 and do a blank run. After doing the baseline corrections, we incubated different concentrations of GSH as 0.1 mM, 0.5 mM, 1.0 mM, 2.0 mM, 4.0 mM, 6.0 mM, 8.0 mM, and 10 mM in the sample cuvette and observed that with the increase in the concentration of GSH, there was a new UV-visible absorption band at 520 nm which was found to be a characteristic peak of the reported iron(III)-salicylate complex. The release of Fe^{+2} in the presence of GSH from **(Fe^{III}T-CATL)$^{3-}$** complex resulted in the formation of $^{\bullet}OH$ radicals via Fenton-like chemistry which reacted with benzoic acid to give salicylic acid and finally formed an iron(III)-salicylate complex.

We have also done a control experiment to confirm that the hydroxyl radical generation is mainly due to **(Fe^{III}T-CATL)$^{3-}$** complex, not by [$Fe(NO_3)_3.9H_2O$] in the presence of GSH. For that, we incubate [$Fe(NO_3)_3.9H_2O$] (0.2 mM), and benzoic acid (0.2 mM), both in the sample and the reference cuvette in 5% DMSO-PBS buffer at pH 7.4 and do a blank run. After doing the baseline corrections, we incubated different concentrations of GSH as 0.1 mM, 0.5 mM, 1.0 mM, 2.0 mM, 4.0 mM, 6.0 mM, 8.0 mM, and 10 mM in the sample cuvette and observed that with the increase in the concentration of GSH, observed no characteristic peak at 520 nm without taking the **(Fe^{III}T-CATL)$^{3-}$** complex**.**

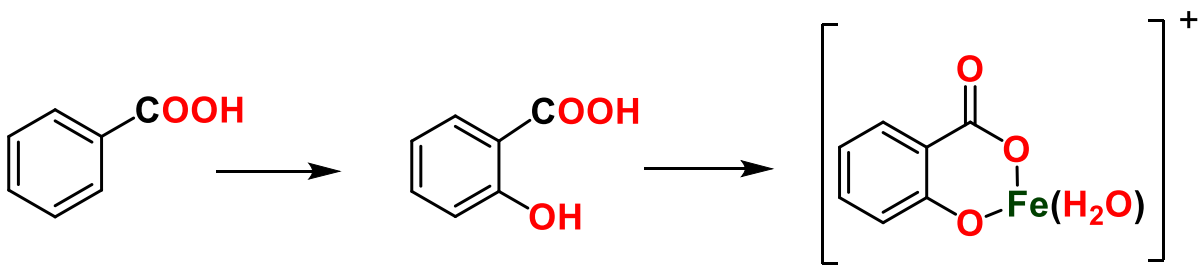

Glutathione Depletion Study (DTNB assay)[10,11]

We have followed a previously published protocol by our group that showed the GSH depletion chemically through UV-visible spectroscopy.[44] The only thing we have modified in the protocol was taking ascorbic acid as a reducing agent to release the unbound iron as Fe^{+2}. We have focused our study on examining the capacity of the **$(Fe^{III}T\text{-}CATL)^{3-}$** complex to deplete glutathione, using Ellman's reagent [DTNB = 5,5'-dithiobis-(2-nitrobenzoic acid)]. DTNB directly reacts with thiols (-OH) groups and can be used to quantify the thiol-containing species in any sample. Reduced glutathione (GSH) contains a thiol (-OH) group and thus directly reacts with DTNB to produce a chromophore TNB (5′-thio-2-nitrobenzoic acid) and a GS-TNB adduct. The chromophore TNB exhibited a strong absorption peak at 412 nm. To measure the total GSH concentration in any sample we initially, generated a standard curve by plotting absorbances at 412 nm (A_{412}) concerning known GSH concentration (0-55 μM). We observed that the rate of change in absorbance at 412 nm is linear, allowing us to conduct linear regression analysis of the standard curve and quantify the total GSH concentration in the unknown samples. Firstly, we incubated 200 μM of ascorbic acid and 55 μM of DTNB in a 5% DMSO-PBS buffer medium (pH= 7.4), to ensure whether the ascorbic acid is reducing DTNB or not. After 10 minutes of incubation, we didn't see any change in the DTNB peak. Then within the same incubation, we added 100 μM of **$(Fe^{III}T\text{-}CATL)^{3-}$** complex and put it in for a further 10 minutes to see any change in DTNB. After seeing no change, we have added 50 μM of GSH. UV-visible spectral traces were taken every 10 minutes of incubation. We have taken ascorbic acid as a reducing reference in place of GSH so that we can show the GSH depletion more specifically. Considering the absorbance values at 412 nm, we calculated the corresponding GSH concentration for each sample from the standard curve. We determined the amount of GSH depleted by subtracting the corresponding GSH concentration from the initial GSH concentration of 50 μM in each sample.

Partition Coefficient Measurements[12]

Lipophilicity is a crucial factor in determining the distribution and tissue permeability of a medication. The partition coefficient was determined by calculating the ratio of the concentration of the ligand (**T-CATL)** in the octanol layer to the concentration in the aqueous layer (P = coct/cwater). The logP represents the logarithm of the partition coefficient, which is the ratio of the concentration of a substance in 1-octanol to its concentration in water. Deionized water was stirred with octanol for 24 h and then centrifuged for 5 min to obtain octanol-saturated water and water-saturated octanol. The ligand (**T-CATL)** was dissolved in the octanol-saturated water, to a typical concentration of 0.03 to 3 mg mL^{-1} and then mixed with water-saturated octanol in volumetric ratios of 1:1, 1:2, and 2:1 in duplicate. The mixtures were vortexed for 0.5 h and then centrifuged for 5 min. The layers were separated carefully using a fine gauge needle and then analyzed for ligand content by UV-visible spectroscopy.

BSA binding[13]

Blood serves as the primary transporter of medications within the human body, with the serum albumin protein playing a key role in delivering the drugs to their intended destination. A protein binding investigation was conducted by doing tryptophan fluorescence quenching tests. Bovine serum albumin (BSA) stock solution, with a concentration of 3 X 10^{-5} M based on its molecular mass of 66000 Da, was used. The experiments were carried out in a 10 mM Tris-HCl buffer with a pH of 7.2 to maintain physiological conditions. With increasing the concentration, the quenching of the emission intensity of tryptophan residues of BSA at ~348 nm was monitored using the ligand (**T-CATL)** 0.003 mM as a quencher. Fluorescence measurements were carried out using a HITACHI F-7000 fluorescence spectrophotometer by keeping the concentration of BSA constant (2 mL, 3 X 10^{-5} M) while varying the quencher concentration at room temperature. A linear fit of the data was done using the Stern–Volmer equation:

$$\frac{I_0}{I} = +kq\tau_0[Q] = 1 + K_{sv}[Q]$$

Cell culture conditions[14]

The Human non-small lung cancer cells (A549), triple-negative breast cancer cells (MDA-MB-231) & human embryonic kidney (HEK293) cells were procured from NCCS (National Centre for Cell Science) in Pune, India. Merck, Millipore, USA provided us with the human cardiac myocyte cell line (AC16). All cells were cultured in Dulbecco's modified Eagle's medium (DMEM) (Gibco, Grand Island, NY, USA) with 10% FBS (Fetal Bovine Serum), 100 U mL^{-1} penicillin and incubated at 37°c in a 5% Co_2 atmosphere.

Cytotoxicity assay (MTT assay)[15]

The cellular toxicity level of the ligand **(T-CATL)** was measured by using the MTT reduction assay. To investigate the impact of our compound of interest on cell growth and proliferation, various cells such as AC-16, HEK293T, A549, and MDA-MB-231 were exposed to varying concentrations of the compound for a period of 36 hrs[3]. Following the cells were seeded at a density of 6×10^4 cells per well in a 96-well plate. Then they were incubated in a CO_2 incubator at 37 °C and 5% carbon dioxide with the culture medium consisting of DMEM + 10% FCS (Gibco). After incubation, the culture medium was replaced and the cells were treated with different concentrations of Ligand compound without phenol red culture medium for 36 hrs. This was followed by preparing 0.5 mg/ml MTT solution in phenol red-free medium adding 10 µl of MTT per well and incubating for 3 hrs. After a 3-hour incubation period, solubilization of water-insoluble formazen 150 µl DMSO was added per well. The optical density (OD) was determined by using a plate reader (Biotek instrument) at a wavelength of 570nm.

DCFDA assay[15]

To assess the intracellular levels of Reactive Oxygen Species (ROS), the cell-permeable oxidation-sensitive test CM-H2DCFDA was performed. A549 & MDA-MB-231 cancer cells were incubated with ligand **(T-CATL)** for 24h. Subsequently, cells were harvested by centrifuged and rinsed twice with cold 1XPBS for 5 mins. CM-H2DCFDA (5μM)[3] was added to cell lysates followed by resuspension in PBS and incubated for 20 mins in the dark at 37°c. Next, the cells were flushed with ice-chilled 1X PBS and lysed utilizing PBS containing Tween20 (1%). The fluorescence of dichlorofluorescein (DCF) was used to determine the generation of intracellular ROS at 480 nm of an excitation wavelength and 530nm of an emission wavelength.

Measurement of Mitochondrial Membrane Potential[15]

Mitochondria membrane potential (MMP, ΨM) was evaluated by monitoring the interaction between mitochondria and fluorescent dye JC-1(5,5',6,6'-tetrachloro-1,1',3,3'-tetraethyl benzimi-dazolylcarbocyanine iodide), following a standard protocol. A459 and MDAMB-231 cells were first grown in FCS (10%) containing DMEM media. Following the treatment with DMSO-PBS (Negative control) and Ligand **(T-CATL)**, the cells were subsequently incubated for a duration of 26 hrs. Cells were collected after the incubation time to quantify the levels of ROS (reactive oxygen species). Then Cell lysates were incubated with dye JC-1 (2.5 μg/mL) in a phosphate buffer solution solution (PBS) at 37 °C for approximately 25-30 mins while being continuously shaken[3]. The cells were then resuspended in PBS after undergoing three times 5-minute washes with cold 1X PBS. Subsequently, the fluorescence intensity ratio at 590 nm to 530 nm was recorded to assess the potential of the mitochondrial membrane.

APOPTOSIS[15]

The Roche cell death detection kit was used to quantify the rate of apoptosis in A549 and MDA-MB-231 cancer cells treated with DMSO-PBS (negative control) and Ligand **(T-CATL)**. The cytoplasmic histone-associated DNA fragments were quantified by using an ELISA kit. The results are shown as a fold increase in the enrichment factor (cytoplasmic nucleosomes)[3].

Annexin-V/FITC Assay[16]

About 4 x 10^5 A549 cells were plated in 96 well plates and grown for 24 h and cells were treated with the ligand **(T-CATL)** (37 μM) for 4 h. The cells were further incubated for 1 h, trypsinized, and washed in DPBS twice. The cells were then re-suspended in 400 μL of 1X binding buffer and 1 μL of annexin V-FITC and 2 μL of PI were added to each cell suspension. These tubes were then incubated at room temperature for 20 min in the dark and the fluorescence of the cells was measured immediately with a flow cytometer. Cells that are early in the apoptotic process were stained with the annexin V-FITC alone while live cells showed no staining by either PI or annexin V-FITC. Late apoptotic cells were stained by both PI and annexin V-FITC while the dead cells were only stained by PI.

Immunoblotting[17]

The treated cells were rapidly frozen in liquid nitrogen and then they were lysed with RIPA buffer (Abcam) containing protease and phosphatase inhibitors (Abcam). The cell lysates were prepared and quantified by BCA assay[4]. After that, 20 μg of protein sample were separated using SDS-PAGE and then transferred onto nitrocellulose/PVDF membrane. Following the transfer, the membranes were blocked for one hour using a 5% BSA solution in 1X TBST. The membrane was washed with 1X TBST for 10 minutes. After blocking, the membranes were incubated overnight with the corresponding primary antibody at 4ºC. The next day, the immunoblots were incubated for 1h with HRP-tagged secondary antibodies after three successive 10-minute washes with 1X TBST. Subsequently, the detection of immunoreactivity was achieved using chemiluminescence. To quantify the densitometry of western blots was done by Image J software (NIH). Here β-actin was used to normalize the amount of protein expressed as a ratio in relation to the control group.

Table S1: Cytotoxicity data (IC_{50}/ µM) obtained from the nonregration analysis of the cell viability plots.				
Compound	**IC_{50} (A549) (µM)**	**IC_{50} (MDA-MB-231) (µM)**	**IC_{50} (HEK293) (µM)**	**IC_{50}(AC16) (µM)**
Ligand (T-CATL)	14.19	20.23	>80	>80

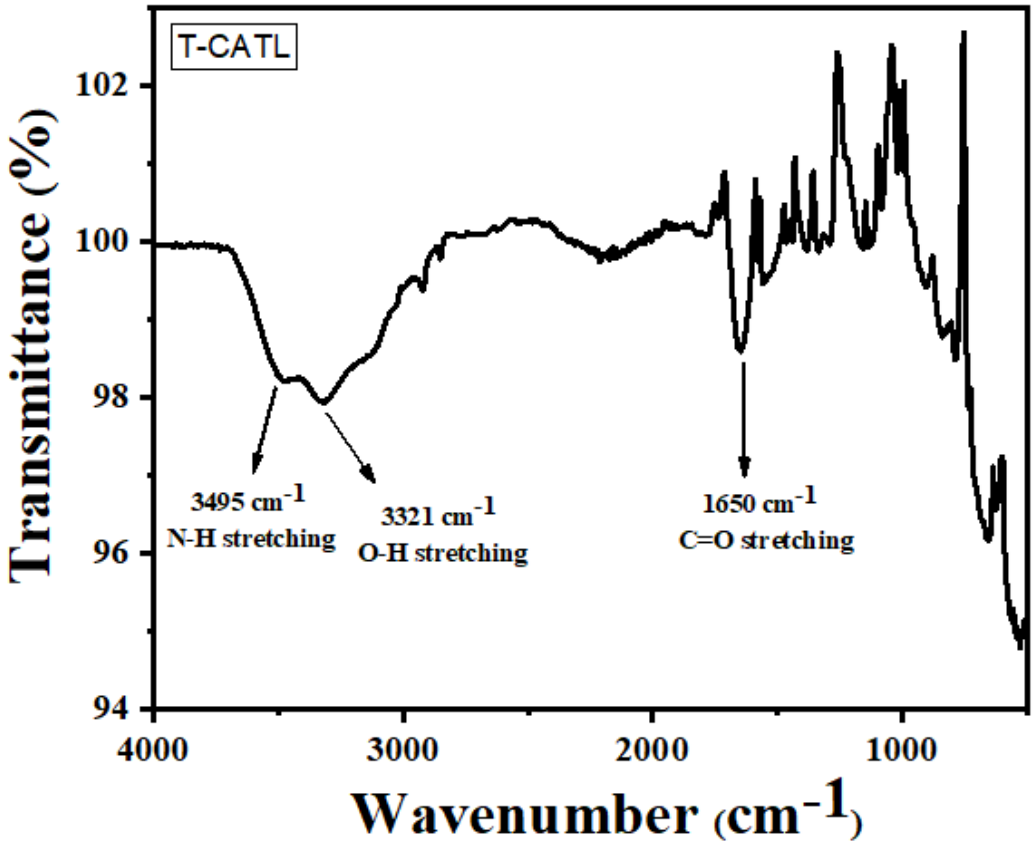

Figure S1. FT-IR Spectra of **T-CATL** recorded in KBr phase using Perkin-Elmer UATR TWO FT-IR Spectrometer.

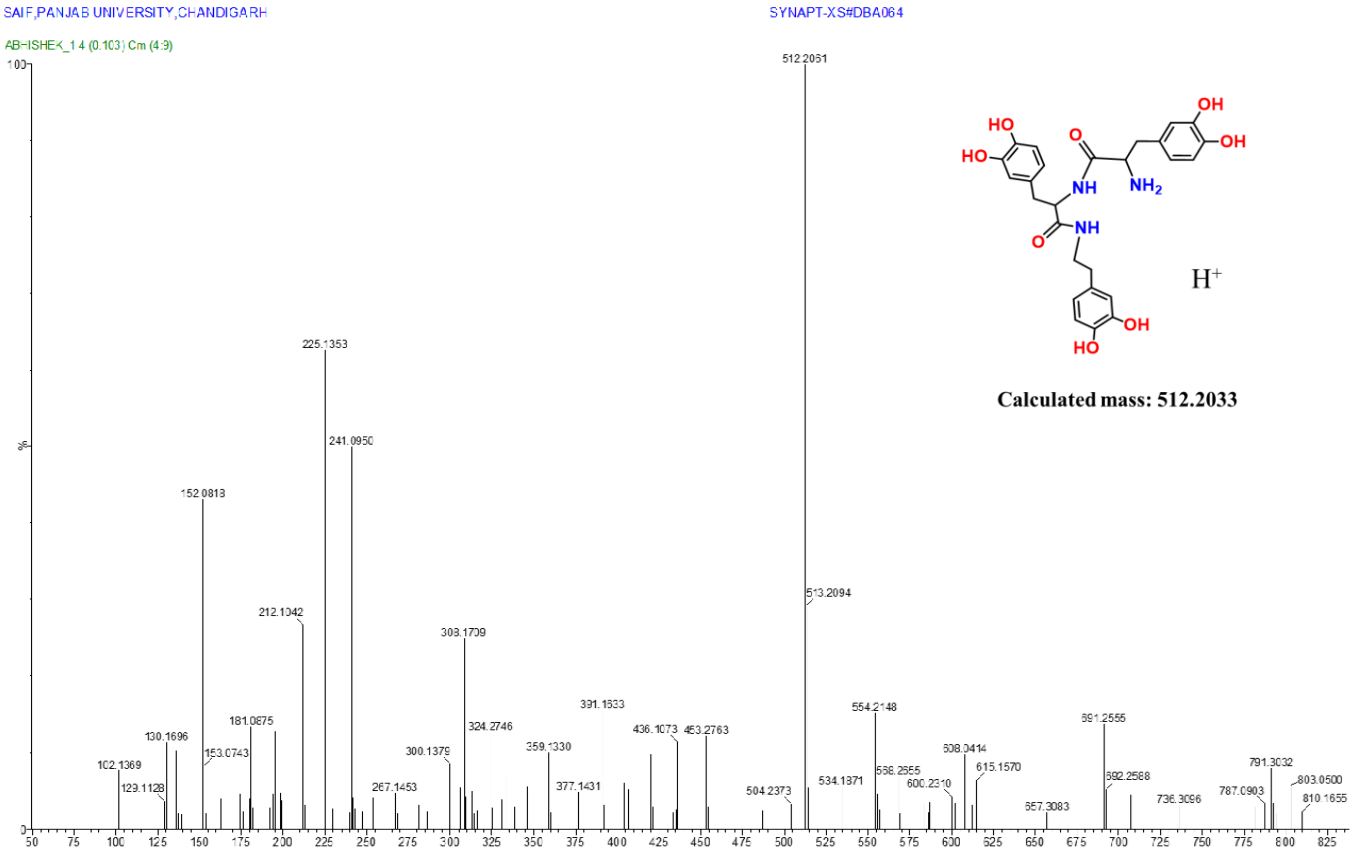

Figure S2: Q-TOF ESI Mass spectra of the **T-CATL** was recorded in CH_3OH using Bruker Esquire 3000 Plus spectro-photometer (Bruker-Franzen Analytic GmbH, Bremen, Germany). The peak at m/z is 512.2061, which corresponds to the species $[T\text{-}CATL\text{-}H]^+$.

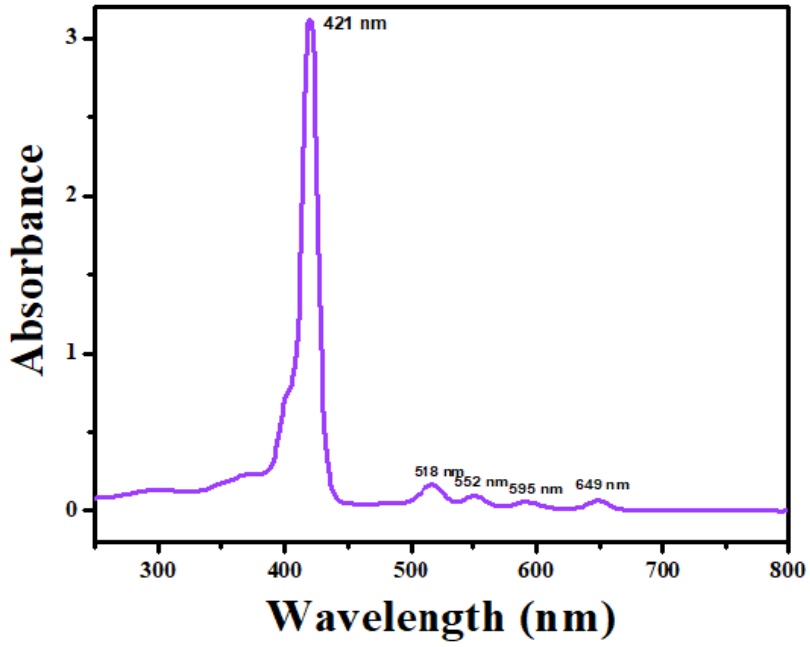

Figure S3: UV-visible spectra of the **TPTP** (0.3 mM) in 5% DMSO-PBS buffer at pH 7.2 in 298 K.

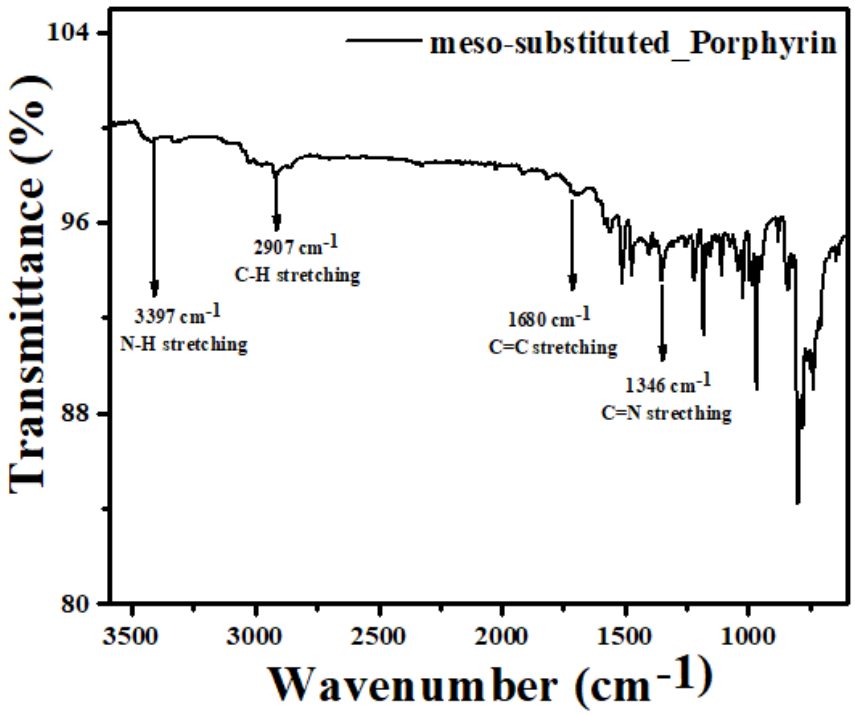

Figure S4: FT-IR Spectra of **TPTP** recorded in KBr phase using Perkin-Elmer UATR TWO FT-IR Spectrometer.

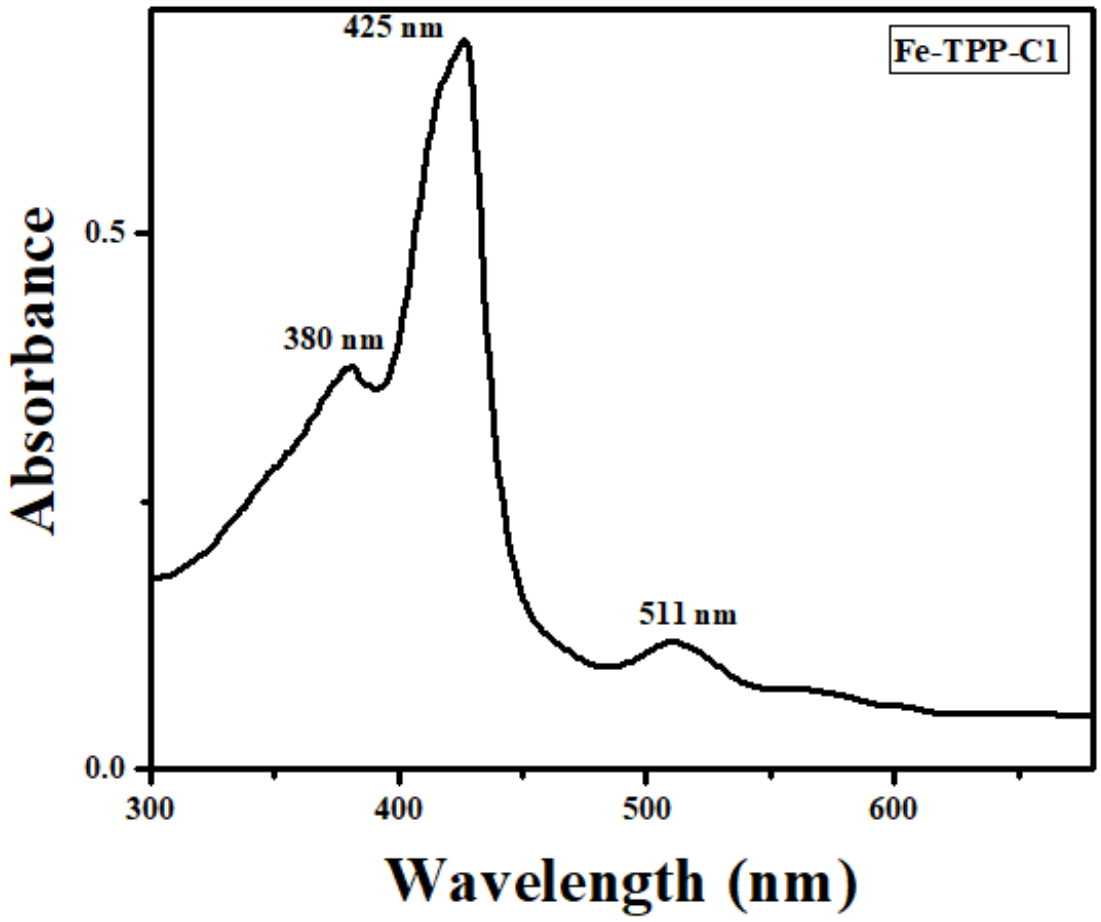

Figure S5: UV-visible spectra of the **Fe-TPP-Cl** (0.03 mM) in 5% DMSO-PBS buffer at pH 7.2 in 298 K.

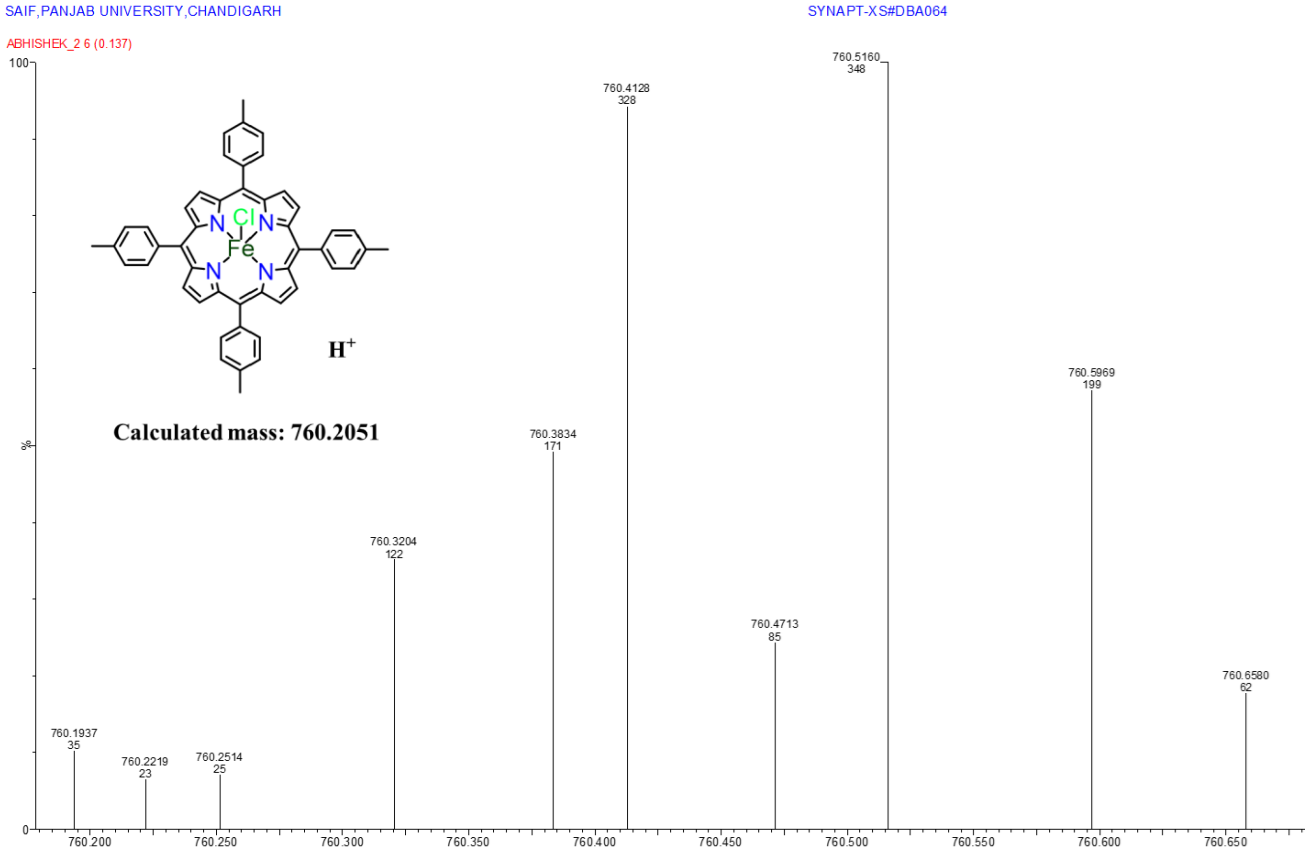

Figure S6: Q-TOF ESI Mass spectra of the **Fe-TPP-Cl** was recorded in DMF using Bruker Esquire 3000 Plus spectro-photometer (Bruker-Franzen Analytic GmbH, Bremen, Germany). The peak at m/z is 760.1937, corresponding to the species $[Fe\text{-}TPP\text{-}Cl\text{-}H]^+$.

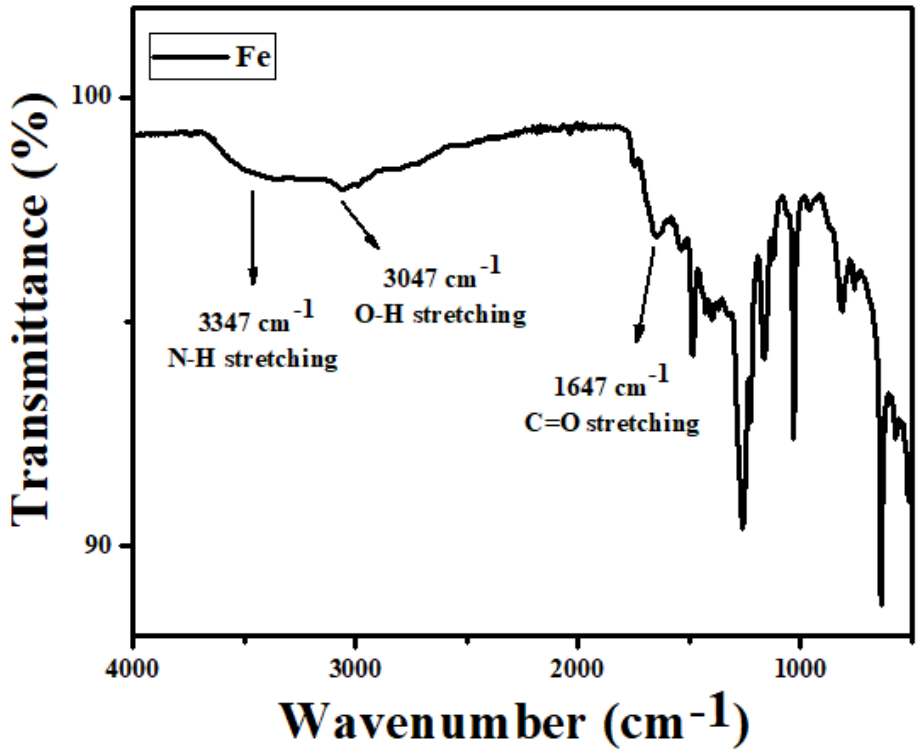

Figure S7: FT-IR Spectra of **$(Fe^{III}T\text{-}CATL)^{3-}$** complex recorded in KBr phase using Perkin-Elmer UATR TWO FT-IR Spectrometer.

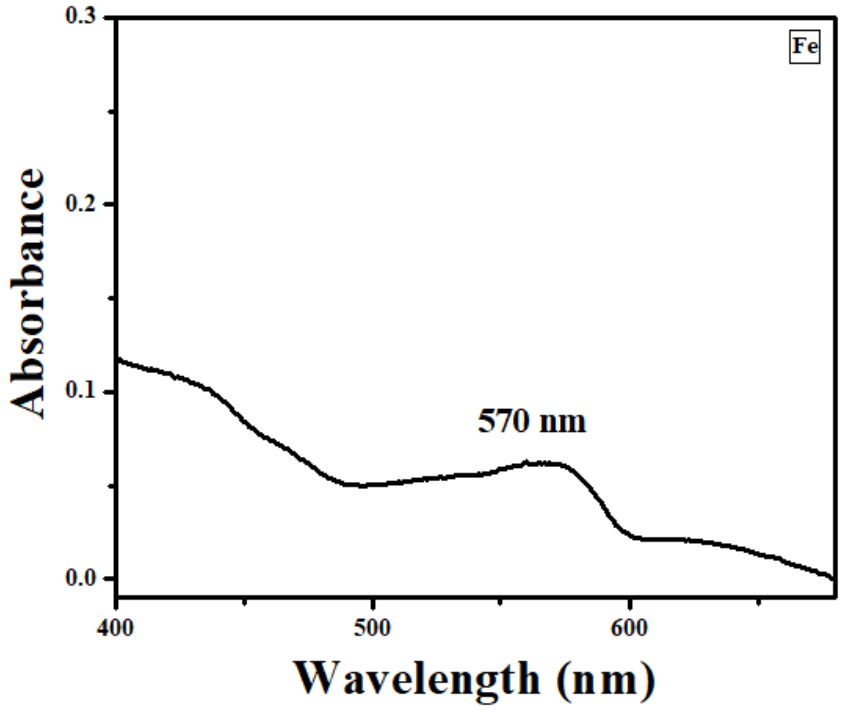

Figure S8: UV-visible spectra of the **$(Fe^{III}T\text{-}CATL)^{3-}$** complex (0.03 mM) in 5% DMSO-PBS buffer at pH 7.2 in 298 K.

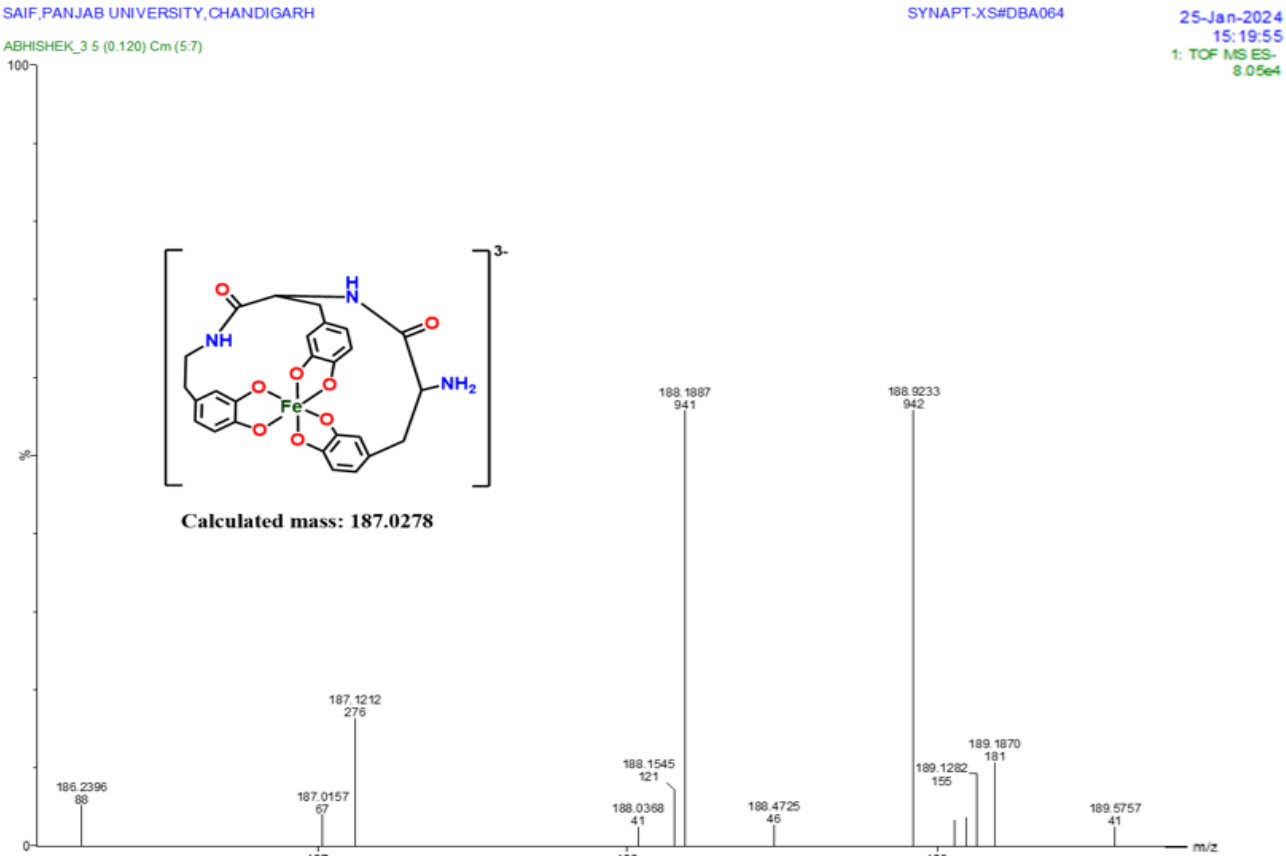

Figure S9: Q-TOF ESI Mass spectra of the **$(Fe^{III}T\text{-}CATL)^{3-}$** complex was recorded in DMF using Bruker Esquire 3000 Plus spectro-photometer (Bruker-Franzen Analytic GmbH, Bremen, Germany). The peak at m/z is 187.0157, corresponding to the species [**$(Fe^{III}T\text{-}CATL)^{3-}$**].

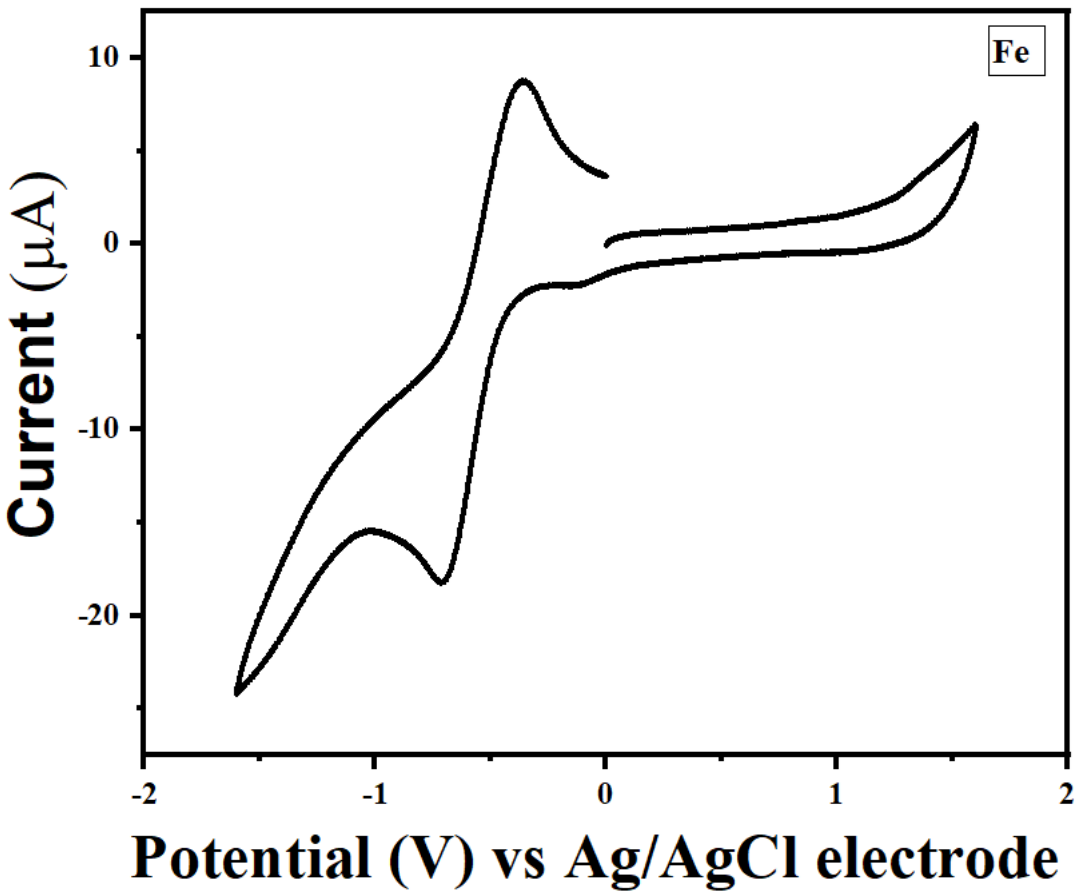

Figure S10: Cyclic Voltammogram of **$(Fe^{III}T\text{-}CATL)^{3-}$** complex, using (0.03mM) solution of **$(Fe^{III}T\text{-}CATL)^{3-}$** complex in DMF at room temperature 298 K using Glassy Carbon electrode as working electrode, Ag/AgCl electrode as reference electrode, and Pt electrode as counter electrode and TBAP (Tetrabutylammonium perchlorate) 0.1 M as supporting electrolyte, scan rate 50 mV/s.

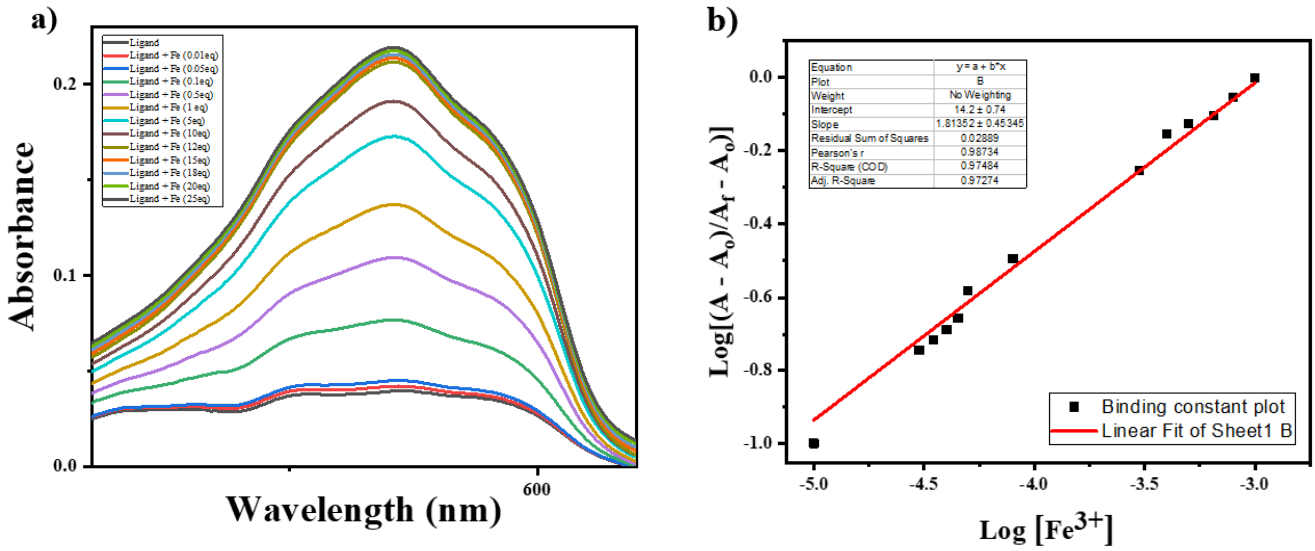

Figure S11: a) UV-visible titrations of aqueous Fe^{3+} ions with a solution of **T-CATL** ligand (0.5 mM) in 5% DMSO-PBS buffer at pH 7.4, room temperature. b) Benesi–Hildebrand plots for determination of binding constant of **T-CATL** for Fe^{3+} ion.

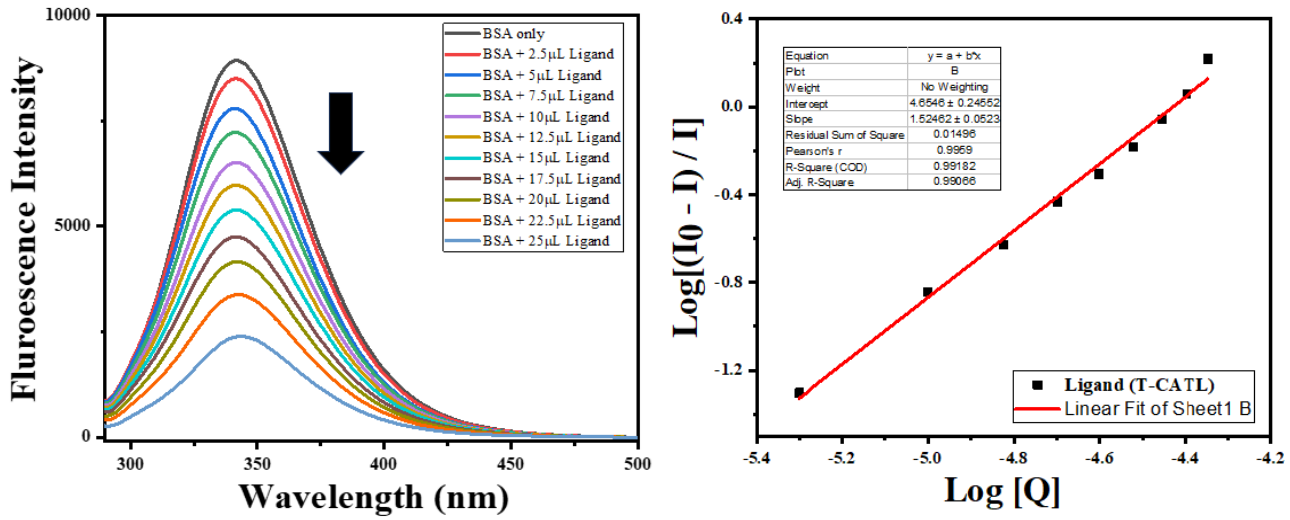

Figure S12: BSA binding studies of (**T-CATL)** (0.3 mM) taking 200 µL BSA from (3×10^{-5} M) stock in Tris-HCl-Buffer (5 mM, pH = 7.2) at room temperature, a Scatchard plot is being added.

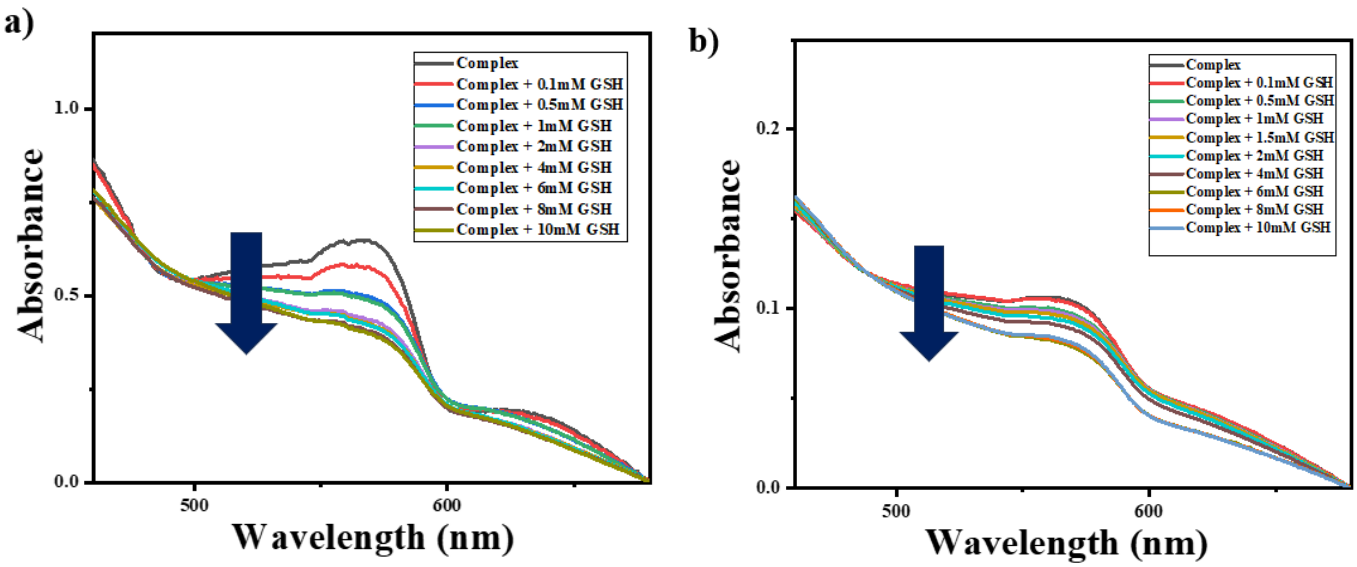

Figure S13: a) Spectroscopic studies of GSH assisted reduction of **$(Fe^{III}T\text{-}CATL)^{3-}$ complex** (0.2mM) upon addition of different concentrations of GSH in a 5% DMSO-PBS buffer at pH5.5 and b) pH 7.4, room temperature which shows degradation of LMCT band around 570 nm indicating the reduction of Iron(III) to Iron(II).

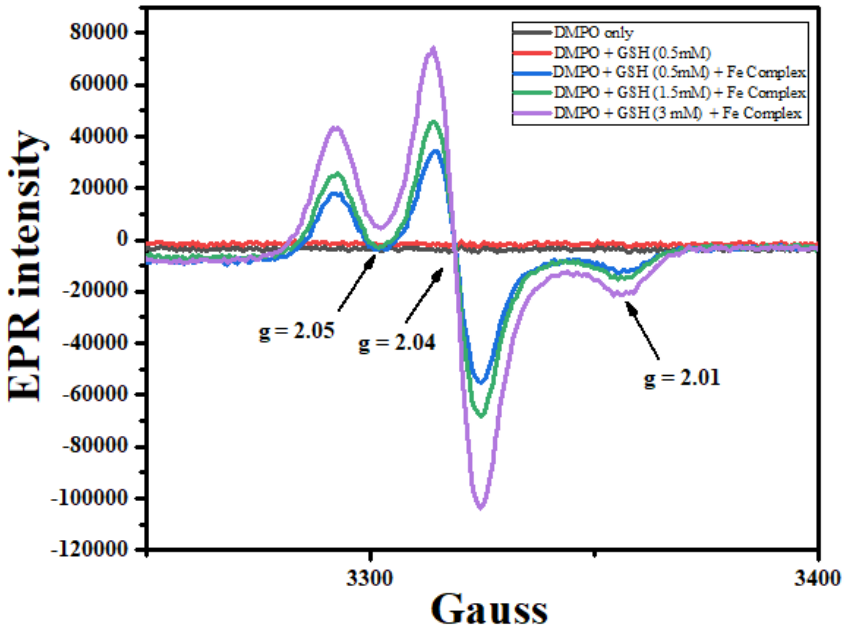

Figure S14: EPR spectra recorded for Hydroxyl radical trapping studies in 5% DMSO–H_2O solution at pH 7.2 and temperature 77 K upon adding different concentrations of GSH on **$(Fe^{III}T\text{-}CATL)^{3-}$** complex**,** using 5,5-dimethyl-1-pyrrolidine (DMPO) as a probe.

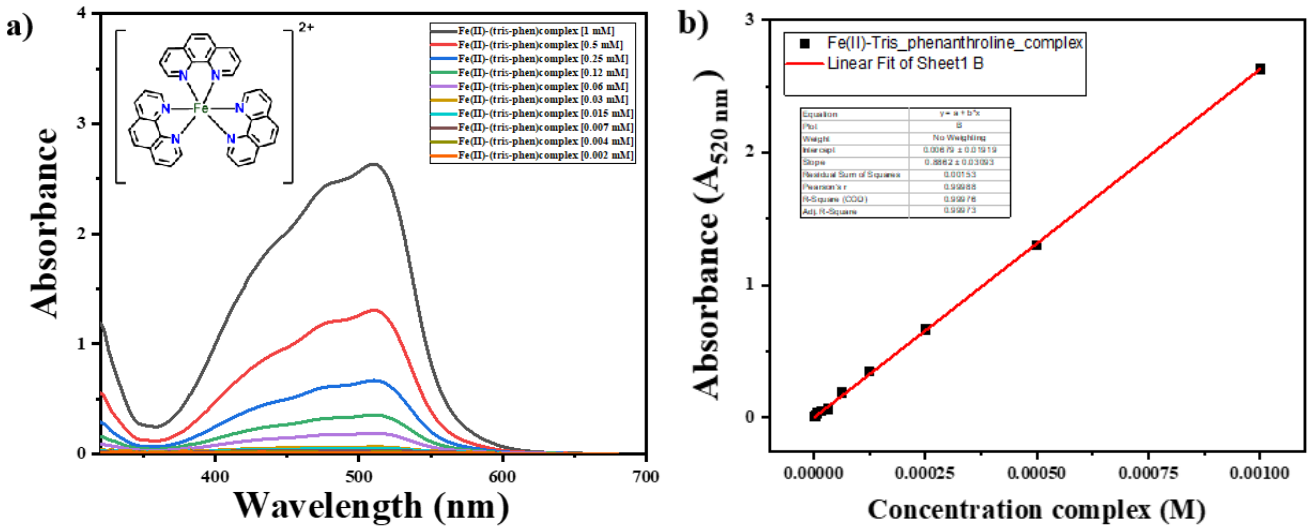

Figure S15: (a) UV-visible spectroscopic studies of **Fe(II)-tris phenanthroline complex** for calculating the percentage release of Fe^{2+} and from the plot we draw a (b) Calibration curve to fit the data.

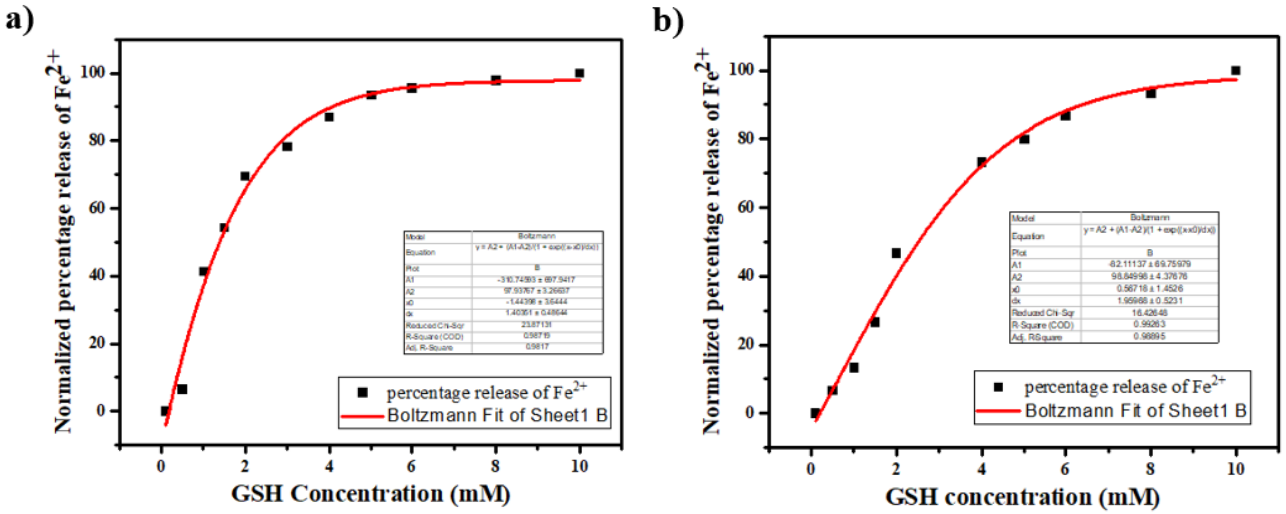

Figure S16: a) Boltzmann curve plot for showing the normalized percentage release of Fe^{2+} from **$(Fe^{III}T\text{-}CATL)^{3-}$** complex in the presence of different concentrations of GSH at pH 5.5 and b) at pH 7.4, and was found to be 83% formation at pH 5.5 while 80% formation at pH 7.4.

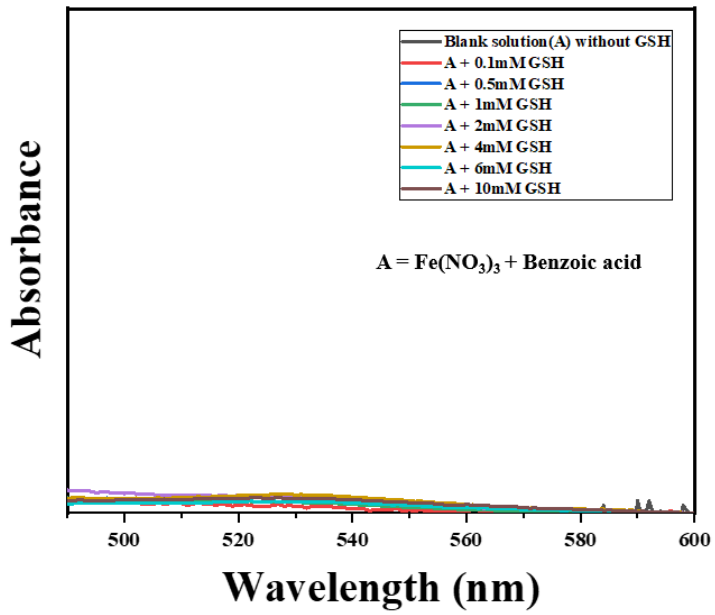

Figure S17: Control experiment for knowing the generation of hydroxyl radical without using **$(Fe^{III}T\text{-}CATL)^{3-}$ complex** through Uv-visible spectroscopic studies in the presence of different concentrations of GSH in a 5% DMSO-PBS buffer at pH 7.4, room temperature.

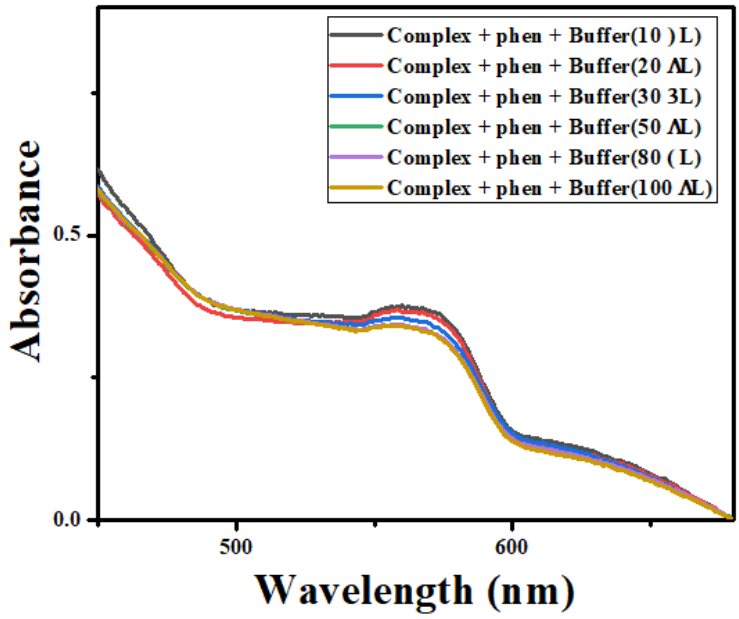

Figure S18: Control experiment for knowing the stability of **$(Fe^{III}T\text{-}CATL)^{3-}$ complex** in the presence of 1,10-phenanthroline through Uv-visible spectroscopic studies upon addition of different concentrations of buffer in a 5% DMSO-PBS buffer at pH 7.4, room temperature.

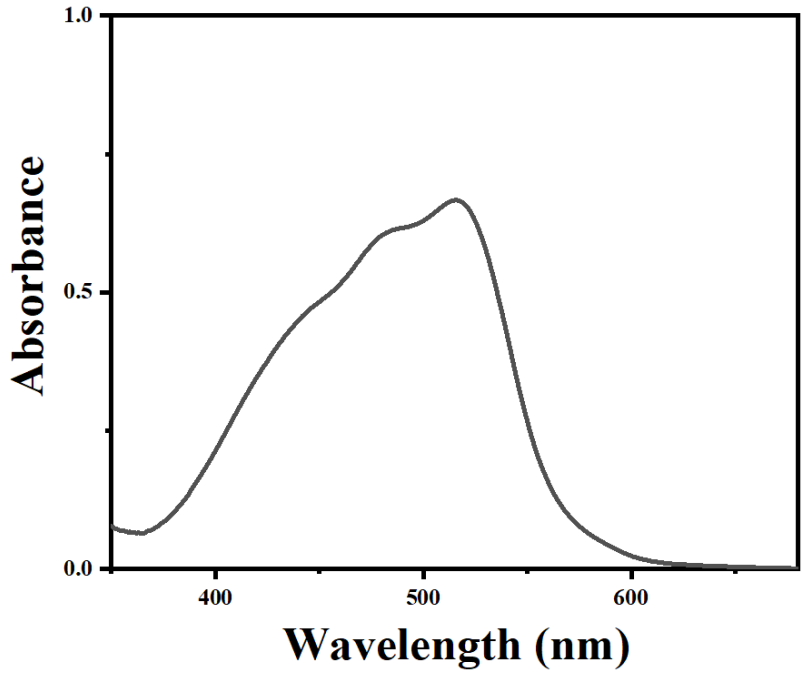

Figure S19: UV-visible spectra of the **[Fe(phen)$_3$]$^{2+}$** complex (0.03 mM) in 5% DMSO-PBS buffer at pH 7.2 in 298 K.

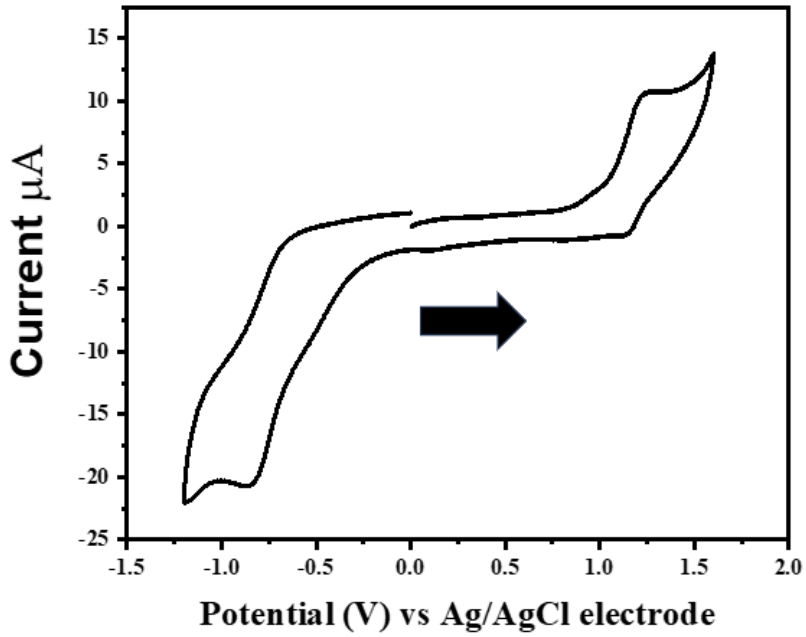

Figure S20: Cyclic Voltammogram of **[Fe(phen)$_3$]$^{2+}$** complex, using (0.3mM) solution of **[Fe(phen)$_3$]$^{2+}$** complex in DMF at room temperature 298 K using Glassy Carbon electrode as working electrode, Ag/AgCl electrode as reference electrode, and Pt electrode as counter electrode and TBAP (Tetrabutylammonium perchlorate) 0.1 M as supporting electrolyte, scan rate 50 mV/s.

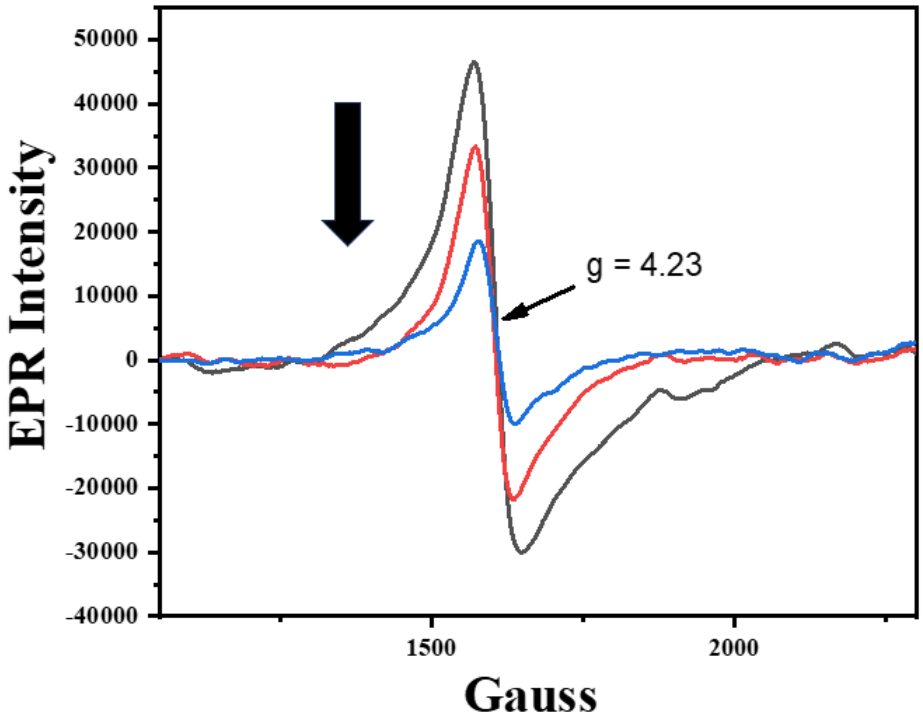

Figure S21: Change in the EPR signal of **$(Fe^{III}T\text{-}CATL)^{3-}$** complex in 5% DMSO–$H_2O$ solution at pH 7.2 and temperature 77 K upon addition of different concentrations of GSH.

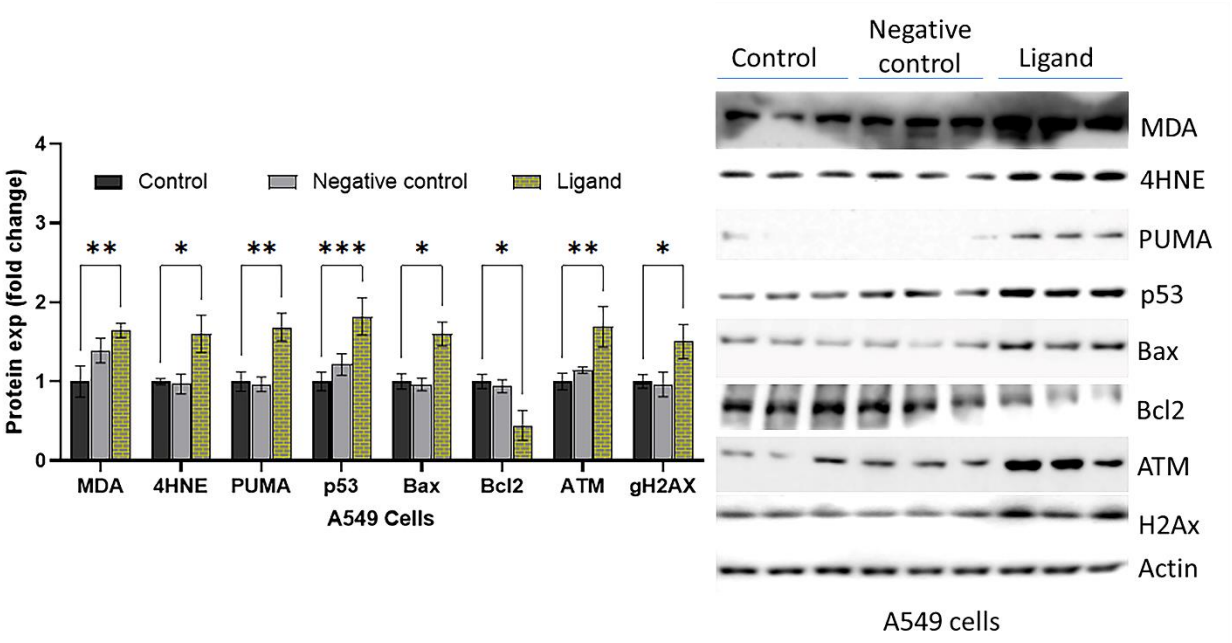

Figure S22: Protein Expression studies of various apoptotic, oxidative stress, and DNA damage markers were documented in A549 cells treated with Ligand **T-CATL** (1µM), DMSO-BSA (as negative control) and untreated (control). For all western blots, β-actin was used as a loading control. All results are represented as means ± S.E. (n=3, *p<0.05; **p<0.01, ***p<0.001, ****p<0.0001 compared to control group).

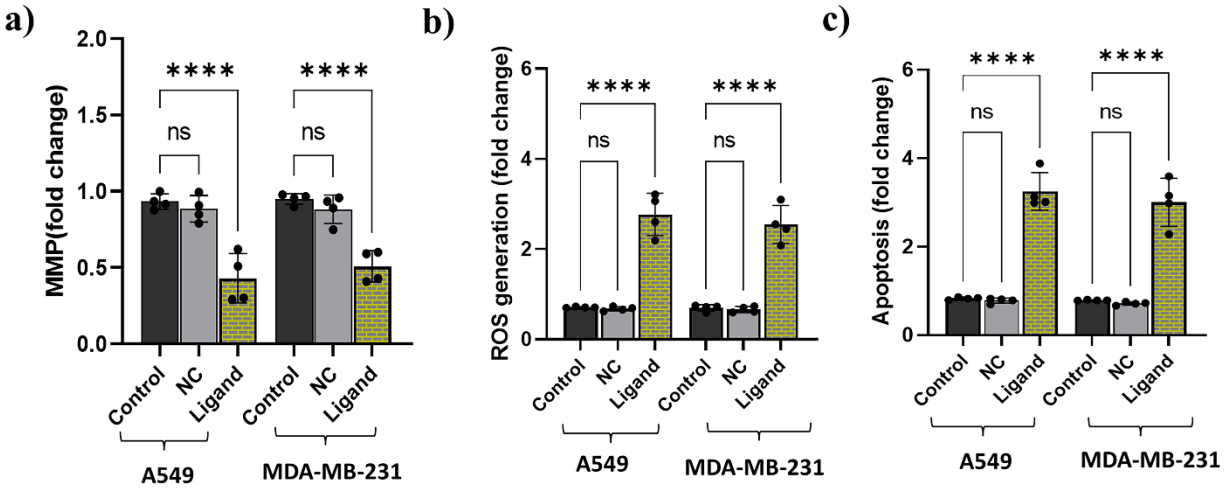

Figure S23: Synthesized compound, Ligand **(T-CATL)** treatment caused mitochondrial and oxidative stress that triggered apoptosis in both A549 & MDA-MB-231 cancer cells. (a) Loss of mitochondrial membrane potential (MMP, $\Delta\psi_m$) was analyzed with control, negative control (cell treated with DMSO-BSA), and Ligand **(T-CATL)**. (b) ROS generation in both A549 and MDA-MB-231 cancer cells. CM-H2DCFDA was used to measure the generation of ROS by fluorescence at 24 hrs. (c) Apoptosis was measured as the rise in fold change in enrichment factor by the formation of cytoplasmic histones-associated DNA fragments. All data are shown as means $\pm$ S.E. (n=4, *p<0.05; **p<0.01, ***p<0.001, ****p<0.0001 compared to control group)

References

1. Pangborn, A. B.; Giardello, M. A.; Grubbs, R. H.; Rosen, R. K.; Timmers, F. J. Safe and Convenient Procedure for Solvent Purification. *Organometallics* **1996**, *15* (5), 1518–1520. https://doi.org/10.1021/om9503712.
2. D. Roy, A. Chakraborty and R. Ghosh, *RSC Adv*., **2017**, 7, 40563–40570.
3. Y. Zhao, X. Cai, Y. Zhang, C. Chen, J. Wang and R. Pei, *Nanoscale*, **2019**, 11, 12250–12258.
4. A. G. Ritacca, E. Falcone, I. Doumi, B. Vileno, P. Faller and E. Sicilia, *Inorg. Chem*., **2023**, 62, 3957–3964.
5. E. Agustina, J. Goak, S. Lee, Y. Seo, J. Park and N. Lee, *ChemistryOpen*, **2015**, 4, 613–619.
6. L. G. Bachas, L. Cullen, R. S. Hutchins and D. L. Scott, *Dalton Trans*., **1997**, 1571–1578.
7. P. Kord Forooshani, R. Pinnaratip, E. Polega, A. G. Tyo, E. Pearson, B. Liu, T.-O. Folayan, L. Pan, R. M. Rajachar, C. L. Heldt and B. P. Lee, *Chem. Mater.*, **2020,** 32, 8182–8194.
8. X. Sui, J. Wang, Z. Zhao, B. Liu, M. Liu, M. Liu, C. Shi, X. Feng, Y. Fu, D. Shi, S. Li, Q. Qi, M. Xian and G. Zhao, *Commun. Biol*., **2024,** 7, 199 DOI:10.1038/s42003-024-05903-5.
9. Gazi, S.; Ananthakrishnan, R.; Semi-Quantitative Determination of Hydroxyl Radicals by Benzoic Acid Hydroxylation: An Analytical Methodology for Photo-Fenton Systems, *Curr. Anal. Chem*., **2012**, (8), 143.
10. Caito, S. W.; and Michael A.; Quantification of glutathione in Caenorhabditis elegans, *Curr. Protoc. Toxicol*., **2015**, 64, 6-18.
11. R. Bhowmik, A. Upadhyay, M. Pal, A. Bera and M. Roy, *New J Chem.*, **2024**, 48, 5465–5474.
12. Wilson, J. J.; and Lippard, S. J.; In Vitro Anticancer Activity of cis-Diammineplatinum(II) Complexes with β-Diketonate Leaving Group Ligands, *J. Med. Chem.*, **2012**, 55, 5326-5336.

13. Shao, J.; Bao, W.G.; Tian, H.; Li, B.; Zhao, X. F.; Qiao, X.; Xu, J.Y.; Nuclease activity and protein-binding properties of a novel tetranuclear thiosemicarbazide Pt(II) complex. *Dalton Trans.*, **2014**, 43, 1663.
14. K. Das, M. Basak, T. Mahata, M. Kumar, D. Kumar, S. Biswas,S. Chatterjee, M. Moniruzzaman, N. C. Saha, K. Mondal,P. Kumar, P. Das, A. Stewart, and B. Maity, RGS11-CaMKIIcomplex mediated redox control attenuates chemotherapy-induced cardiac fibrosis, *Redox Biol*., **2022**, 57, 102487.
15. S. Sivagnanam, K. Das, M. Basak, T. Mahata, A. Stewart,B. Maity and P. Das, Self-assembled dipeptide based fluorescent nanoparticles as a platform for developing cellular imaging probes and targeted drug delivery chaperones, *Nanoscale Adv*., **2022**, 4, 1694–1706.
16. Musib, D.; Pal, M.; Raza, M. K.; Roy, M.; Photo-physical, theoretical and photo-cytotoxic evaluation of a new class of lanthanide(iii)–curcumin/diketone complexes for PDT application. *Dalton Trans*., **2020**, 49 10786-10798.
17. M. Basak, K. Das, T. Mahata, A. S. Sengar, S. K. Verma,S. Biswas, K. Bhadra, A. Stewart and B. Maity, RGS7-ATF3-Tip60 Complex Promotes Hepatic Steatosis, and Fibrosis by Directly Inducing TNFa, Antioxid. *Redox Signaling*, **2023**, 38,137–159.